LAWRENCE
LIVERMORE
NATIONAL
LABORATORY

UCRL-JRNL-230147

High-Power Laser Pulse Recirculation for Inverse Compton Scattering-Produced Gamma-Rays

I. Jovanovic, M. Shverdin, D. Gibson, C. Brown

April 20, 2007

Nuclear Instruments and Methods in Physics Research A

Updated October 14, 2003

High-Power Laser Pulse Recirculation for Inverse Compton Scattering-Produced Gamma-Rays

I. Jovanovic *, M. Shverdin, D. Gibson, and C. Brown

Lawrence Livermore National Laboratory, Mail Code L-270, 7000 East Avenue, Livermore, CA 94550, USA

Abstract

Inverse Compton scattering of high-power laser pulses on relativistic electron bunches represents an attractive method for high-brightness, quasi-monoenergetic γ-ray production. The efficiency of γ-ray generation via inverse Compton scattering is severely constrained by the small Thomson scattering cross section. Furthermore, repetition rates of high-energy short-pulse lasers are poorly matched with those available from electron accelerators, resulting in low repetition rates for generated γ-rays. Laser recirculation has been proposed as a method to address those limitations, but has been limited to only small pulse energies and peak powers. Here we propose and experimentally demonstrate an alternative method for laser pulse recirculation that is uniquely capable of recirculating short pulses with energies exceeding 1 J. Inverse Compton scattering of recirculated Joule-level laser pulses has a potential to produce unprecedented peak and average γ-ray brightness in the next generation of sources.

Key words: Inverse Compton scattering, laser recirculation, monoenergetic gamma-rays
PACS: 01.30.−y

1 Introduction

Inverse Compton scattering (ICS) exhibits some favorable characteristics not present in other methods for generation of x-rays and γ-rays, such as directionality and quasi-monochromaticity [1]. The resulting potential for high

* Corresponding author
Email address: jovanovic1@llnl.gov (I. Jovanovic).

brightness of sources based on ICS is of significant interest for numerous applications, including high-energy physics [2], nuclear transmutation and spectroscopy [3,4,5,6], and medical diagnostics and treatment [7,8]. The projected brightness of such sources increases nonlinearly with the photon energy [9], which significantly improves their brightness and utility at energies >1 MeV.

In addition to the monochromaticity and directionality, other desired characteristic of ICS-produced γ-rays include high peak power (photon number in unit time per pulse) and high average power (repetition rate). High peak power is desirable in applications that require good temporal resolution, such as time-resolved radiography, as well as in applications in which reduced integration time may produce improved signal-to-noise ratio. High average power would be of great benefit in applications in which the integrated energy (photon number) delivered to the sample is essential, such as nuclear transmutation/spectroscopy and medical applications. In those applications high average power reduces the operation time or alternatively increases the scanning rate.

ICS-based γ-ray sources are based on the combination of two different technologies: electron accelerators and high-energy short-pulse lasers. The relativistic electron bunches are normally generated by conventional linear electron accelerators [2,10], preferrably equipped with low-emittance photoinjectors. High-energy short laser pulses can be produced by modern solid-state chirped-pulse amplification systems [11]. In the recent period, some convergence of two technologies has occured with the demonstration of monoenergetic laser-based electron accelerators [12], with increasing prospects for their use in all-laser-driven γ-ray production via ICS [13].

In the ICS interaction, the small Thomson scattering cross section limits the efficiency of conversion of incident laser photons to γ-rays. Typical backscattered fraction of the incident photons is $<10^{-9}$, so that the ICS interaction region is essentially transparent to laser photons. Furthermore, a significant technology gap in repetition rate exists between linear accelerators and high-energy short-pulse lasers. While the linear accelerators are capable of producing electron bunches in bursts with repetition rates of $\sim$GHz, typical joule-level short-pulse lasers are limited to $\sim$10-Hz repetition rates.

Recirculation of the laser pulse has been previously proposed as a method to bridge some of this technology gap. For the future International Linear Collider (ILC), 2820 micropulses in a macropulse are proposed, generated by resonant cavity build-up and recirculation [14,2]. Recirculation of high-energy short pulses by resonant cavity coupling requires interferometric alignment accuracies and requires high-energy laser sources with high repetition rates, or the use of multiple such sources.

In this paper we propose and experimentally demonstrate a novel method for

high-energy laser pulse recirculation based on the injection and trapping of a single incident laser pulse in a passive optical cavity, akin to "burst-mode" operation. This method circumvents the B-integral limitations of conventional optical switching by the use of a thin nonlinear switch based on frequency conversion in a nonlinear crystal. Following the nonlinear pulse injection, subsequent recirculation is shown to be capable of increasing the average power and brightness of ICS-based γ-ray sources by a factor of $\sim$100. Further, this recirculation method, termed recirculation injection by nonlinear gating (RING), is scalable to >100-J picosecond pulses, well beyond the capability of alternative recirculation methods.

In addition to the proof-of-principle experimental demonstration, we provide the estimate of the effect of RING recirculation on the spectral and spatial characteristics of the recirculating pulse, of relevance for the characteristics of generated γ-rays. It is also shown how the RING method can be applied to generation and recirculation of tunable laser pulses, as well as for simultaneous recirculation of multiple laser frequencies, which can enable simple tunable or polychromatic γ-ray sources. The use of RING is compatible with the current paradigm of ICS-based γ-ray sources, offering a significant improvement in average power and possible reduction in laser energy and electron accelerator energy. The concept is complementary to the much costlier development of higher repetition rate lasers, and it could also be used in conjunction with higher repetition lasers when they become available.

2 Laser recirculation methods and limitations

Laser recirculation has been used for numerous applications, primarily motivated by the need for higher power output. The use of laser recirculation is intertwined with the development of the resonant cavity which enables the laser action itself. Approaches to laser recirculation demonstrated to date can be classified by several criteria, and here we mention some of the important examples, their features and limitations.

Intra-cavity components can include only passive elements which result in power (energy) loss and rely on external coupling of the light. Alternatively, a cavity can also include a gain element such as a laser or a parametric device, which can compensate for the cavity power loss [15]. For most ICS applications of interest, the recirculated laser pulse is short and the required pulse energy is high, which is incompatible with direct amplification in a compact laser amplifier due to spectral and spatial modification of the propagating pulse. The nonlinear phase accumulation (B-integral) due to self-phase modulation of the medium from an intense optical pulse can be written as

$$\phi^{(2)}(x,y) = \frac{2\pi}{\lambda}\int_0^L n_2 I(x,y,z)dz, \tag{1}$$

where $\phi^{(2)}$ is the accumulated B-integral, λ is the laser center wavelength, n_2 is the nonlinear refractive index of the material, $I(x,y,z)$ is the pulse intensity, and L is the length of the medium along pulse propagation direction z. In a typical laser amplifier, the accumulated B-integral per pass is incompatible with direct amplification and recirculation of a short energetic laser pulse. In such cases the use of chirped-pulse amplification [11] would be preferable, but would require a sensitive, complicated setup exhibiting average power limitations due to intra-cavity pulse stretching and compression.

Passive optical cavities are designed to exhibit minimum loss and require continuous or pulsed coupling of an external laser source into the cavity via resonant cavity coupling [16] or via a dedicated optical switch [17]. In resonant coupling, a stringent phase requirement exists for the light incident into the cavity for the constructive interference to occur. For cw light, this corresponds to the incident light spectral overlap with existing cavity modes. For pulsed light, the phase of the incident pulse needs to match the phase of the recirculating pulse and the repetition rate of the incident pulses needs to be identical or a subharmonic of the recirculating pulse. These interferometric requirements correspond to sub-100 nm positioning of optical components for optical frequencies. In a non-resonant coupling scheme, an optical switch such as an electro-optic or acousto-optic modulator can be used to actively modulate the pulse using an external electric or magnetic field [17], or modulate the properties of the switch itself to trap the pulse in the cavity. Conventional linear switches require interaction lengths of several cm and thus encounter the problem identical to active cavities when used with energetic short laser pulses. For even modest pulse energies, the required apertures of such switches that result in acceptable nonlinear phase accumulation are prohibitively large.

From a beam path point of view, the laser can be recirculated in an angularly multiplexed or a collinear scheme. The examples of the former approach include the high-power multipass "bow-tie" laser amplifiers and white cell-like devices, while the latter approach is associated with typical laser and parametric oscillators and regenerative amplifiers. While the angularly multiplexed laser pulses can be injected into the cavity without the use of an optical switch, the number of available recirculation passes is limited and the pulse propagates through the interaction region with a different angle on each pass, which can pose significant difficulties for ICS applications.

3 Recirculation injection by nonlinear gating (RING)

Since the principal limitation that prevents the injection and the recirculation of an intense laser pulse in the cavity is the nonlinear phase accumulation with each passage of the pulse through the relatively thick switching components, one can consider alternative methods for pulse injection that reduce the nonlinear phase. Here we propose a novel method of optical switching into the cavity that requires significantly shorter interaction lengths than the previously used methods and is thus compatible with recirculation of an intense laser pulse. We refer to this concept as recirculation injection by nonlinear gating (RING).

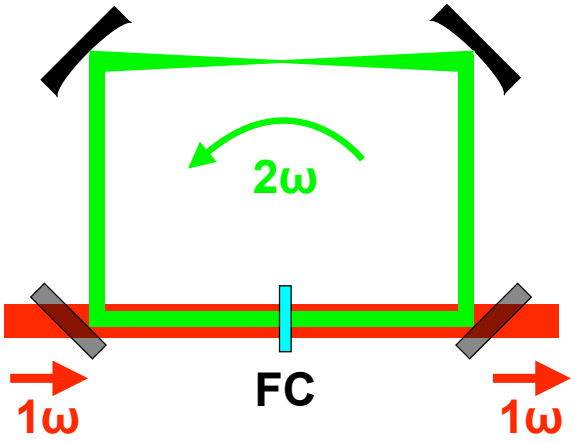

Fig. 1. Optical switching for recirculation in RING is performed by placing a thin frequency converter (FC) into the cavity. The nonlinear crystal frequency converter acts like an optical switch by altering the frequency and polarization of the incident pulse. The cavity is resonant for the frequency and polarization of the frequency converted pulse, and highly transmissive for the frequency and/or polarization of the incident pulse. Parasitic parametric fluorescence produced by the recirculated pulse can be efficiently coupled out of the cavity at each cavity mirror.

The principle of the RING technique is presented in Fig. 1. In the RING technique, optical switching is achieved by placing a thin frequency converter, such as a nonlinear optical crystal, into the cavity so that it is in the path of the incident laser pulse. The frequency converter represents an ideal optical switch - it alters both the frequency and the polarization state of the incident pulse, allowing simple selection and containment of the generated pulse for recirculation by means of dichroic mirrors and polarizers. The thickness of the nonlinear crystal optical switch is determined by the requirement for high conversion efficiency in frequency mixing. For frequency doubling (sum-frequency generation of the incident pulse with itself), this efficiency is approximately given by

$$\eta_{2\omega} = \frac{8\pi^2 d_{eff}^2 I_\omega L^2}{\epsilon_0 n_{2\omega} n_\omega^2 c \lambda_\omega^2}, \tag{2}$$

where $\eta_{2\omega}$ is the conversion efficiency, I_ω is the input pulse intensity, L is the length of the nonlinear crystal, ϵ_0 is the dielectric constant, λ_ω is the wavelength of the incident pulse, and n_ω and $n_{2\omega}$ are the refractive indices of nonlinear crystal for the fundamental and the second harmonic wavelength, respectively. In a typical nonlinear crystal such as β-barium borate (BBO), $d_{eff} \approx 2$ pm/V for frequency doubling of 1064-nm laser pulses. If we assume a typical incident pulse intensity of 5 GW/cm^2, the required length of the crystal for efficient conversion (switching) is only ~3 mm (Fig. 2), which is substantially less than linear optical switches. The RING technique offers a unique advantage of the short interaction length of the pulse in a material, and is thus highly appropriate for short (picosecond and femtosecond) pulses.

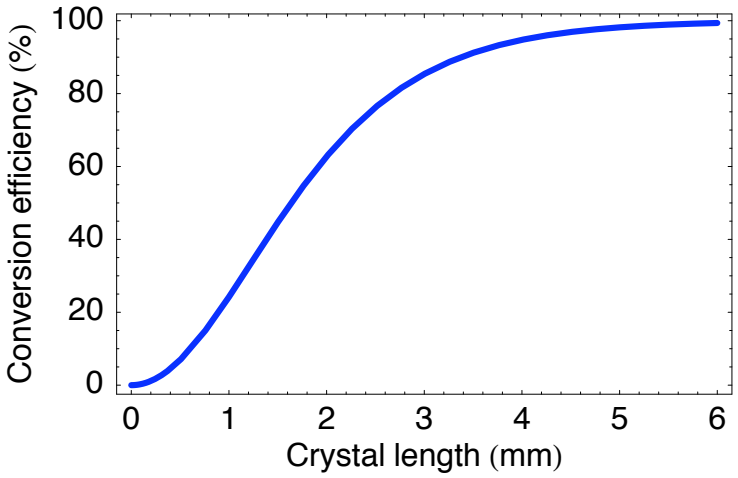

Fig. 2. Conversion efficiency in BBO as a function of crystal thickness. The input peak intensity is 5 GW/cm^2, and the input center wavelength is 1064 nm.

The mode of operation of a RING resonator can be termed a burst-mode, characterized by both high peak and average power. The intra-cavity pulse structure consists of a train of intense short pulses spaced by the cavity round-trip time and exhibiting a decay with characteristic decay time determined by total cavity losses. The entire decaying set of pulses is similar to a macrobunch proposed for the ILC and its repetition rate is determined by the driving laser repetition rate. The recirculated pulse energy for a total cavity loss of 1% per pass is shown in Fig. 3(a).

We can define the cavity enhancement factor as the ratio of the integrated recirculated power and the power produced by nonlinear frequency conversion following the first passage of the incident pulse through the optical switch:

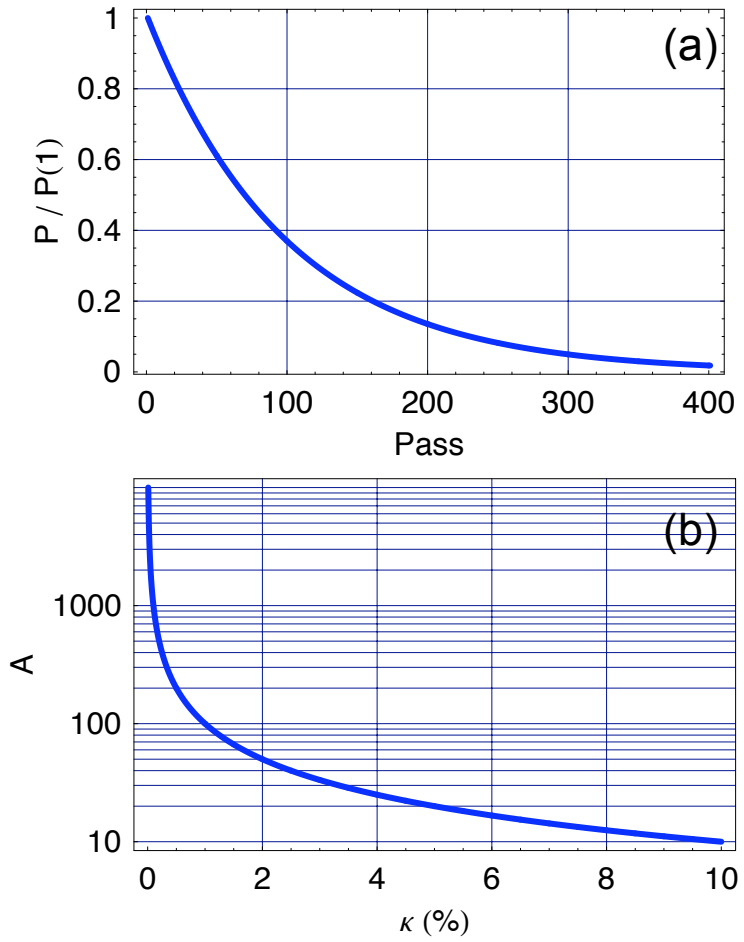

Fig. 3. (a) recirculated pulse energy per pass normalized to the energy in the first recirculation pass for total intra-cavity loss of 1%, and (b) dependence of the cavity enhancement factor on the total intra-cavity loss.

$$A = \frac{\sum_{i=1}^{\infty} P(i)}{P(1)}, \tag{3}$$

where A is the cavity enhancement factor and $P(i)$ is the pulse power in i-th cavity pass. For the example shown in Fig. 3(a), the resulting cavity enhancement factor is 100, which indicates that under identical pulse-to-pulse ICS interaction conditions, the output γ-ray yield would be enhanced by a factor of 100 compared to the one produced by a single-pulse interaction. The cavity enhancement factor is a strong function of the single-pass cavity loss. If we denote the single-pass cavity loss with κ, the cavity enhancement factor is

$$A = \frac{1}{\kappa} = \frac{Q}{2\pi}, \tag{4}$$

where Q is the usual cavity Q-factor. For a reasonable cavity loss of 3% arising from interaction with 6 surfaces with 0.5% loss per surface in each cavity roundtrip, one could expect the cavity enhancement factor of ∼34.

The burst-mode of operation offers a unique advantage of not sacrificing the peak power of the source, while resulting in a significant improvement of the system average power. Furthermore, the use of the RING technique in conjunction with frequency doubling as the switching mechanism conveniently doubles the ICS γ-ray energy without the commensurate increase in the electron energy, leading to potential cost savings of the electron accelerator module of the system.

Similar to other recirculation techniques, the Q-factor of the RING cavity increases with the reduction of Fresnel and scattering loss on each intra-cavity optical surface and the reduction of the total number of surfaces encountered by the pulse. In addition, the RING cavity requires low absorption and Fresnel loss on the nonlinear crystal switch, which can be accomplished by selecting crystals with high transparency and coating them with anti-reflection coatings. Minimization of the number of passes through the nonlinear crystal switch results in a minimum impact of B-integral on the recirculated pulse. For a pulse with a single intra-cavity interaction point (focus), at least one pass through the nonlinear crystal is required per interaction pass.

The RING cavity can be realized in a unidirectional ring or a Fabry-Perot configuration. In both cases the frequency conversion of the input pulse provides optical isolation from the pump laser. In a simple Fabry-Perot configuration, bidirectional propagation of the recirculated pulse offers the possibility of two interactions with the electron bunch per one cavity round-trip; however, one pass through the nonlinear crystal is still required per ICS interaction.

The RING cavity used for ICS exhibits several important requirements: (1) it requires a collimated beam at the location of the nonlinear crystal to produce high frequency conversion efficiency; (2) subsequent passes through the nonlinear crystal should not produce high intensity through reduced beam waist or hot spots to prevent crystal damage; and (3) an interaction point with a focused laser beam is required in the cavity. In addition to these requirements, ICS interactions frequently call for head-on (collinear) interaction geometries, which usually requires a small hole in one or more cavity mirrors to facilitate the passage of the electron beam. Such holes can present a mechanism for cavity loss for most cavity modes. One of the straightforward methods that results in self-reproducing beam sizes and transverse distributions is relay imaging.

Relay imaging leads to a self-imaged cavity, with each cavity component experiencing constant (or inverted) intensity distribution on each pass of the recirculated pulse. The matrix transfer function M of such self-imaged system in a planar geometry is:

$$M = \begin{pmatrix} (-1)^p & 0 \\ 0 & (-1)^r \end{pmatrix}, \tag{5}$$

where $p, r = \pm 1$. The self-imaged cavity allows the use of apertures (holes) in the cavity optics, while maintaining a low loss per pass.

It is useful to consider the energy and interaction point intensity scaling of the RING cavity. With the selected thickness of the nonlinear crystal switch, the required pulse intensity and fluence on the nonlinear crystal are fixed by the requirement for high conversion efficiency (2). In a simple RING configuration shown in Fig. 1, the f-number ($f/\#$) of intra-cavity focusing is determined by the focal length of the focusing lens (reflective mirror or parabola) and by the size of the beam. A smaller beam on the focusing optic is undesirable due to relatively high intensity of the pulse undergoing frequency conversion in the nonlinear crystal. The peak power P incident on the nonlinear crystal is proportional to the square of the beam (crystal) diameter D: $P \propto D^2$, while $f/\# \propto 1/D$. The resulting focal spot intensity at the interaction point is thus proportional to the fourth power of the beam diameter:

$$I \propto \frac{P}{w^2} \propto D^4. \tag{6}$$

In this simple cavity configuration, the two strategies for obtaining the desired focal spot intensity are thus (1) modification of the focal length of the focusing lens (leading to the modification of cavity length), and (2) ICS operation at a variable distance from focus.

4 RING nonlinear spectral effects

As stated earlier, one of the key parameters that determines the performance of the RING technique is the B-integral accumulation. In this section we consider the impact of B-integral on the spectrum of the recirculated pulse and estimate its effect on the energy spectrum of the γ-ray produced by ICS. B-integral

results in spectral broadening and can thus reduce the spectral brightness of the γ-ray source. It is important to quantify B-integral and develop strategies for B-integral reduction. The origin of the B-integral is primarily the transit of the intense short pulse through the nonlinear crystal. In Fig. 4 we show the calculated B-integral for a typical case of a 3-mm long BBO crystal repeatedly irradiated by pulses in a ring down profile shown in 3(a), with the initial pulse intensity of 5 GW/cm^2. The accumulated B-integral in this configuration is 15.6 for the infinite number of passes. The crystal thickness is chosen to be 3 mm to ensure good conversion efficiency to the second harmonic (Fig. 2).

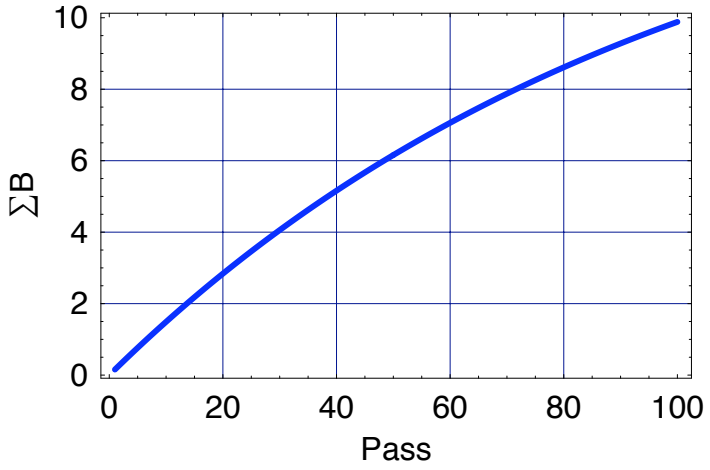

Fig. 4. Accumulated B-integral in 3-mm long BBO crystal irradiated by 532-nm pulses shown in Fig. 3(a), with a starting intensity of 5 GW/cm^2. The assumed nonlinear refractive index of the BBO crystal is $n_2 = 8.8 \times 10^{-16}$ cm^2/W.

The exact nature of the effect of B-integral and dispersion has been modeled using a split-step Fourier method, with nonlinear phase treated in the temporal domain and the linear phase (dispersion) treated in the frequency domain. Fig. 5 displays the evolution of the spectral and temporal shape of a sample incident pulse. For the selected transform-limited bandwidth of the pulse of 5 ps, the effect of dispersion on pulse duration is negligible and a major effect on the pulse spectrum can be observed.

The effect of spectral broadening of the recirculated laser pulse on the resulting peak γ-ray brightness can be analytically evaluated using the formalism of Hartemann *et al.* [9] For a typical spectrum produced by ICS of a 1-μm, 5-ps laser pulse on a 250-MeV electron bunch, the resulting spectrum can be narrower than 1% FWHM for high-emittance, loosely focused electron beams (Fig. 11, bottom in Ref. [9]). For this same example, Eq. (50) in [9] can be used to evaluate the reduction of peak brightness due to B-integral accumulation by approximating the spectral profile of the laser by a gaussian with a variable width. The result of this calculation is shown in Fig. 6 and indicates that the spectral broadening represents a negligible contribution to brightness when the spectral width of the pulse is $<20\times$ pulse transform limit. With the realization

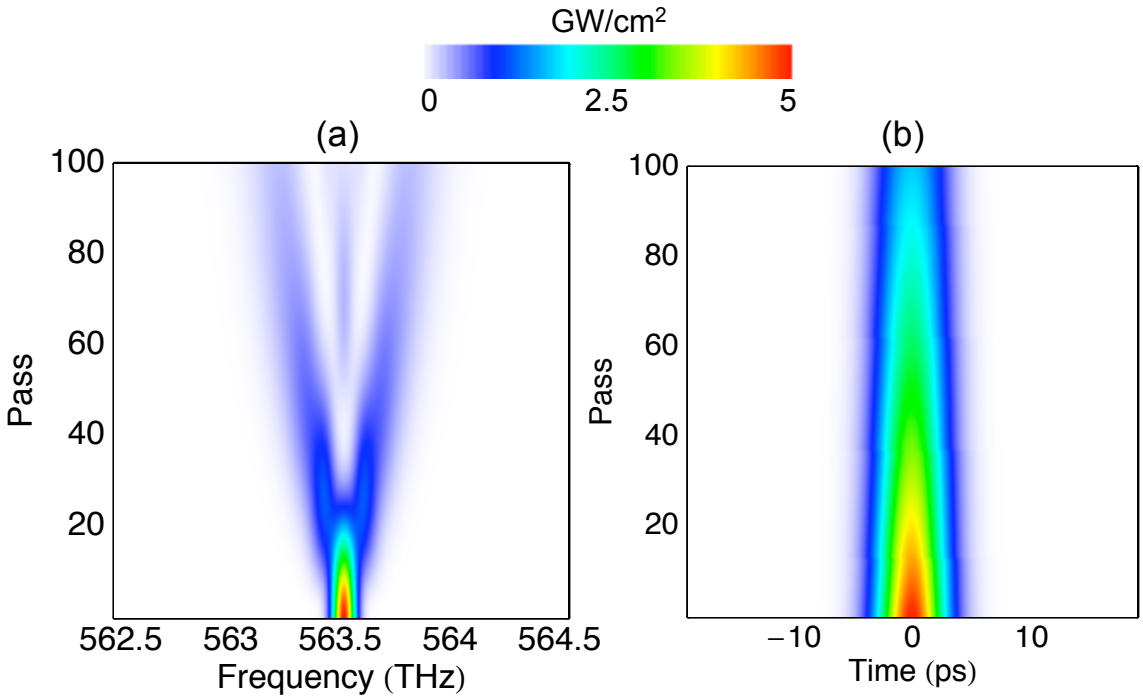

Fig. 5. Effect of B-int on (a) spectrum and (b) pulse duration. The pulse parameters are identical to Fig. 4. The effect of B-integral can be primarily observed in the pulse spectrum after 20-th roundtrip through the cavity.

of spectrally narrower ICS-based γ-ray source, this effect may become more pronounced.

Given the nature of the nonlinear switching process which is accomplished by use of $\chi^{(2)}$ (quadratic) component of dielectric susceptibility, and the subsequent $\chi^{(3)}$ (cubic) nonlinear phase accumulation, an important consideration in nonlinear material selection is the identification of the material with a largest ratio of $[\chi^{(2)}]^2/\chi^{(3)}$, thus allowing good frequency doubling conversion efficiency while simultaneously limiting the accumulation of B-integral. The second strategy for reduction of B-integral effects that emerges is the increase if beam diameter: since we have

$$B \propto I \times L \quad \text{and} \quad \eta \propto I \times L^2, \tag{7}$$

a reduction in intensity coupled with increase in crystal length while keeping the efficiency constant reduces the B-integral. This amounts to the increase in beam aperture and crystal diameter. Practical limits to this strategy include spectral bandwidth limitations of the nonlinear conversion process and available crystal sizes.

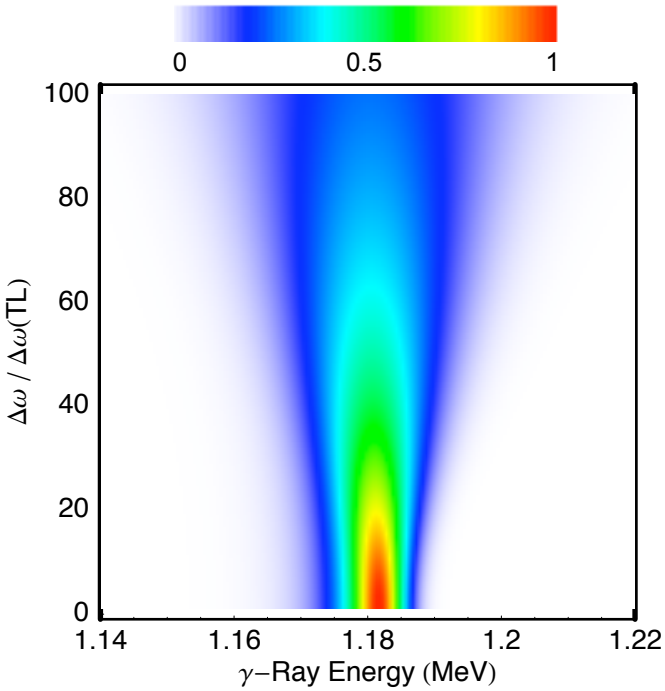

Fig. 6. Calculated effect of B-integral on peak spectral brightness of generated γ-rays at the center energy of 1.18 MeV, with other interaction parameters given in [9]. Only a negligible effect of the spectral broadening on the γ-ray spectral brightness is observed before the spectral broadening exceeds 20×Fourier transform limit.

5 RING nonlinear spatial effects

Spatial variation of accumulated nonlinear phase can have a deleterious effect on the the quality of beam focus and lead to self-focusing. Spatially varying nonlinear phase is the result of $\chi^{(3)}$-nonlinear coupling of the high-power, non-uniform beam profile of a laser beam with the medium (nonlinear crystal or air). In Fig. 7 we show the calculated effect of spatial nonlinear phase on pulse focusing. It is apparent that for the typical set of laser parameters the resulting beam focus can increase significantly over the typical number of passes in the RING cavity.

The impact of this effect on the generated number of ICS γ-rays can be estimated by calculating the cross-correlation of the electron bunch with the recirculating laser pulse:

$$N_s = \sigma c \int_{\vec{r}} \int_t (1 - \vec{\beta}_e \vec{k} \frac{c}{\omega}) N_\gamma(\vec{r}, t) N_e(\vec{r}, t)\ d^3\vec{r}\ dt, \tag{8}$$

where σ is the Thomson scattering cross section, c is the speed of light, ω is the frequency of the incident laser pulse, $\vec{r}$ is the position vector, t is time, $\vec{\beta}_e$ is the electron β-vector, $\vec{k}$ is the incident photon wave vector, and N_γ and N_e

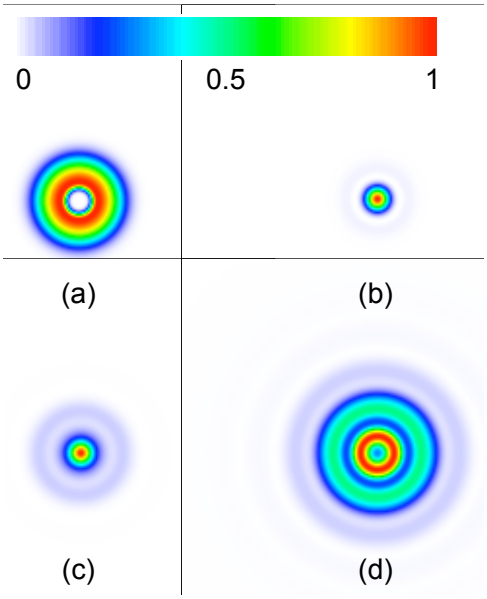

Fig. 7. Effect of spatial B-integral in a 3-mm long BBO crystal on focusing: (a) near field, (b) pass 1, (c) pass 10, (d) pass 20. The input intensity is 5 GW/cm^2, loss per cavity pass is 1%, and the near field of the pulse is approximated by a gaussian profile with a center hole for electron beam passage. All figures are normalized to their respective peak intensities; the actual relative intensity in beams (b)-(d) decreases.

are the incident laser photon and electron number distributions, respectively. Here we assume interaction of the laser pulse with a far-field beam profile resulting from focusing of a holey near-field beam, as shown in Fig. 7, with a representative electron bunch. In this simplified analysis it is assumed that the spatial distributions of the interaction laser pulse and the electron bunch are constant for the entire time of each interaction (confocal beam parameters are not taken into account). The resulting normalized number of ICS γ-ray photons per pass and the cavity enhancement factor are shown in Fig. 8. It is apparent that the increase in focal spot size due to spatial variation in B-integral is the chief contributor to reduced brightness of ICS γ-rays through the reduction of scattered number of photons due to the mismatch in laser and electron bunch focal spot size.

Given that the number of scattered laser photons is much reduced due to the increase in the laser focal spot size, strategies can be considered to progressively reduce the size of focal spot on subsequent passes in the RING cavity by reducing the numerical aperture. An additional benefit of this approach may be due to the energy loss on each pass which would also reduce the number of scattered photons. A simple approach that would allow progressive reduction of the spot size in a self-imaging cavity would be to design the cavity such that its ray transfer matrix departs from identity. Single-pass magnification of the beam prior to interaction with the cavity mirror can be made consistent with the required increase in the numeric aperture to match the foci of the

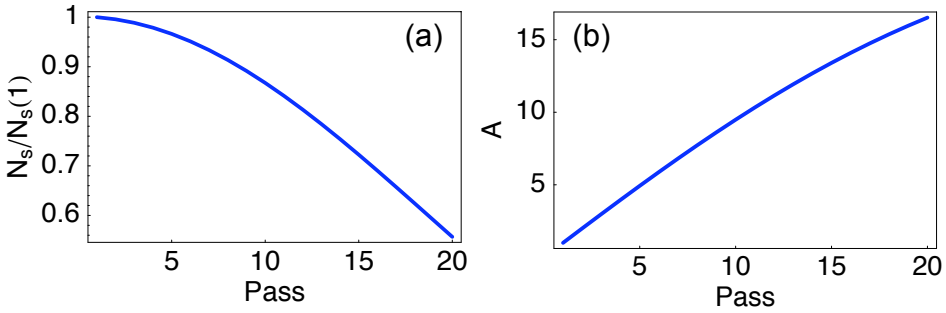

Fig. 8. (a) Normalized number of backscattered γ-ray photons and (b) cavity enhancement factor resulting from the ICS of the focused laser pulse shown in Fig. 7 and a representative electron bunch. Electron bunch exhibits a gaussian distribution with a focal diameter of 20 μm. The number of γ-ray photons is normalized to the number of photons obtained from the first ICS interaction. The laser initial beam diameter is 10 μm.

electron bunch and the laser pulse.

An additional concern can be the whole-beam self-focusing induced by the B-integral. The focal length of the nonlinear lens induced by a spherical phase differential ϕ can be approximated by:

$$f = \frac{w_0^2 - 3(\phi\lambda/2\pi)^2/4}{\phi\lambda/2\pi}, \tag{9}$$

where f is the nonlinear lens equivalent focal length, w_0 is the beam radius, ϕ is the accumulated B-integral, and λ is the center wavelength. For the center wavelength of 532 nm, accumulated nonlinear phase $\phi = 10$ rad, and the beam radius of 10 cm, the equivalent focal length is >10 km, which indicates that only a small change of the focal spot location is expected due to this effect.

6 Experimental demonstration of the RING technique

We have performed initial experiments to establish the feasibility of the RING technique and gain confidence in its scaling to high pulse energies and peak powers by aperture increase. For the demonstration experiment we utilized a simple triangular plane ring resonator configuration (Fig. 9) without intracavity focus, avoiding the need for a vacuum system. The resonator consisted of three high-quality plane mirrors. The mirrors were coated on the side internal to the cavity with a multilayer dielectric coating reflective for the 527 nm wavelength (R>99.9%) and transmissive for the 1053 nm wavelength. The multilayer dielectric coating on the mirror sides external to the cavity is antireflective for both the 1053 nm and the 527 nm wavelength (R<2.1% and

R<0.1%, respectively). This coating selection enables the following functionality: (1) low loss at the resonator wavelength of 527 nm, (2) efficient coupling of 1053 nm light into the cavity, (3) efficient removal of the fundamental 1053-nm light and parametric fluorescence from the cavity, and (4) improved diagnostics of 527 nm recirculated pulse by mirror leakage.

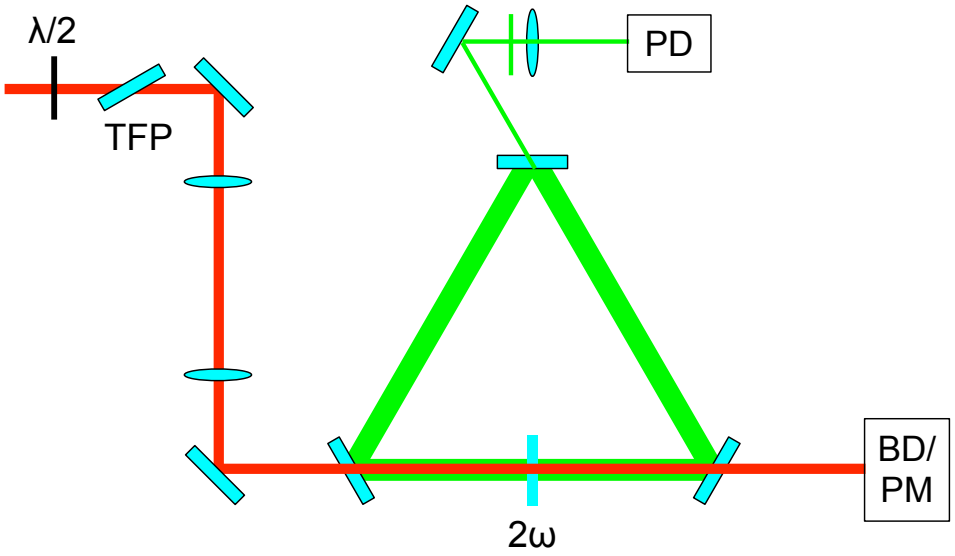

Fig. 9. Experimental setup of the proof-of-principle experiment for demonstration of the RING technique. TFP-thin film polarizer, $\lambda/2$-waveplate, 2ω-BBO crystal doubler, PD-photodiode, BD/PM-beam dump/power meter.

The resonator length was approximately 107 cm, yielding a roundtrip time of 3.6 ns. The use of plane-mirror resonator leads to diffraction losses, but it is estimated that they would negligible over the maximum expected number of ∼100 cavity roundtrips with the selected beam diameter of ∼7 mm and a smooth beam profile.

In two experiments we used two variable-thickness, 1-cm aperture nonlinear crystals of BBO for nonlinear switching. The selection of the BBO crystal for this task is motivated by its numerous favorable properties in nonlinear optics applications. They include excellent thermomechanical properties, low hygroscopicity, and broad spectral and thermal acceptance. The two nonlinear crystals were cut for type I SHG of 1064 nm pulses, antireflection coated on both sides, and their lengths were 3 mm and 1 mm. The 3-mm long BBO crystal antireflection coating was found to be somewhat lossy for the 527 nm frequency doubled light, while the 1-mm crystal coating reflectivity was <1% on both crystal sides. The injected 10-Hz, 1053-nm pulse energy was ∼2 mJ, and the pulse duration was 500 fs, longer than the Fourier transform of the pulse spectrum of 200 fs. The calculated intensity of the pump pulse on the crystal was 10 GW/cm^2. The first-pass frequency doubled pulse energy was measured to be 0.5 mJ with a 3-mm crystal and ∼0.3 mJ with a 1-mm crystal.

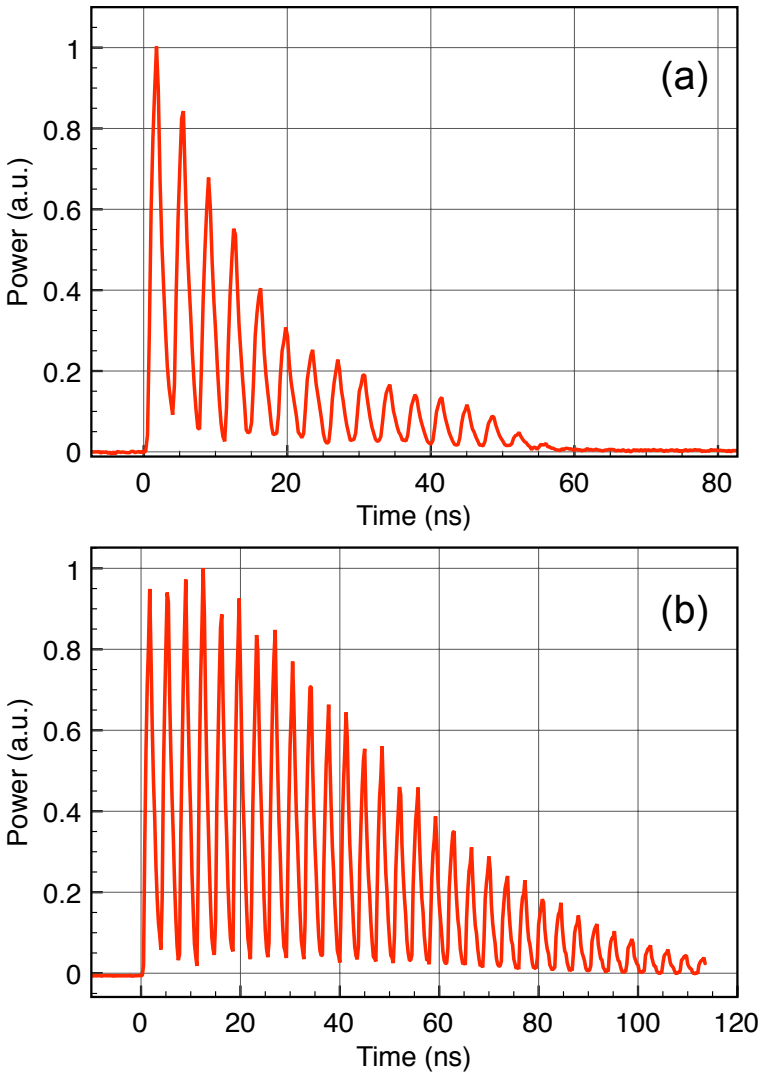

Fig. 10. Cavity ringdown in the proof-of-principle experiment measured using a 1-ns rise time photodiode, using (a) 3-mm long and (b) 1-mm long BBO crystal nonlinear switch. The corresponding cavity enhancement factor is calculated to be 5.2 and 17, respectively. In case (b) the ringdown shape departs from the expected exponential, likely due to the significant increase in hard-edge diffraction losses after the first few cavity round-trips.

The recirculated pulse burst was measured using a 1-ns rise time photodiode combined with a 7-GHz digital oscilloscope by observing the leakage of the 527-nm pulse through one of the cavity mirrors and by measuring the 527-nm scatter from cavity mirrors and the nonlinear crystal surface. The experimentally measured cavity ringdown is shown in Fig. 10 (a) and (b) for the 3-mm and the 1-mm long BBO crystal, respectively. In the case of the 3-mm long crystal, the poor quality of the crystal antireflection coating limited the cavity enhancement factor A to 5.2. In the case of the 1-mm crystal, the improved coating resulted in $A \sim$17. These enhancement factors correspond to approxi-

mately 19% and 6% loss per cavity pass, likely limited by hard-edge diffraction by imperfectly collimated beam and the crystal antireflection coating. Our first proof-of-principle experiment provides the first demonstration of the validity of the technique and increases confidence in the success of its scaling to high energies at similar pulse intensities.

7 Tunable and polychromatic extensions of the RING technique

It has been already pointed out that the simple implementation of the RING technique which involves laser pulse frequency doubling for pulse injection leads to the increase of the resulting ICS γ-ray by a factor of 2, or, equivalently, to the reduction of the required electron energy to produce the same backscattered γ-ray energy. In some applications it may be of interest to recirculate multiple laser pulses centered at different frequencies, or to recirculate pulses which can be conveniently and rapidly tuned in frequency. In medical diagnostics and treatment via x-ray induced Auger electron cascade [7,8], for example, it would be advantageous to rapidly tune the x-ray energy to optimize the system performance. In nuclear spectroscopy applications such as the ones based on nuclear resonance fluorescence [6], frequency scanning of the backscattered γ-rays is of essence for accessing nuclear resonances of desired isotopes and could be conveniently implemented by scanning the laser frequency rather than the electron energy. Additionally, simultaneous recirculation of multiple frequencies and subsequent production of various γ-ray energies may allow simultaneous access to several resonances associated with multiple isotopes or a single isotope. Such methods could increase the speed and sensitivity of proposed spectroscopic techniques and even perhaps open a window to multi-photon nuclear interactions. In plasma diagnostics via Thomson scattering, suitable modification of the laser frequency could improve the signal-to-noise ratio. In cavity ring-down spectroscopy, the need for frequency scanning of the recirculating laser pulse is apparent.

Nonlinear optical processes represent a convenient method for production of pulses at multiple frequencies or for tuning of the light frequency via the processes such as sum- or difference-frequency generation (SFG or DFG). The RING technique which involves the use of a nonlinear optical switch thus represents a natural framework for the use of nonlinear optical processes for production and recirculation of tunable and polychromatic pulses.

A simple implementation of the RING technique for generation and recirculation of tunable laser pulses is shown in Fig. 11. Two pulses at frequencies ω_1 and ω_2 are incident in the RING cavity and frequency mixed in the nonlinear crystal via SFG ($\omega_3 = \omega_1 + \omega_2$) or DFG ($\omega_3 = \omega_1 - \omega_2$). If one or both of the incident frequencies $\omega_{1,2}$ are made tunable, the resulting output pulse can be

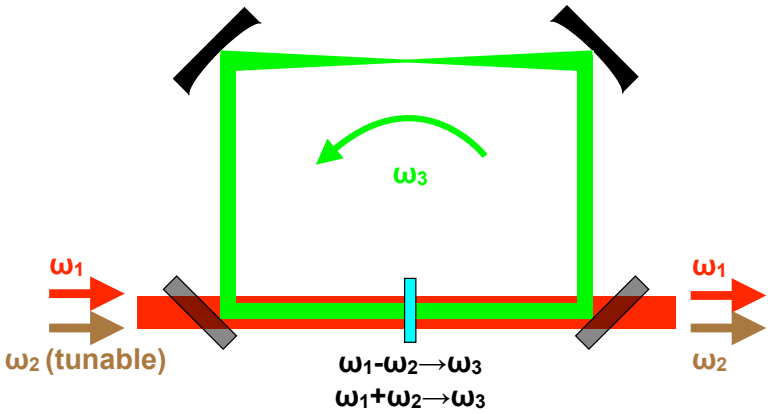

Fig. 11. Tunable RING by SFG or DFG between two incident pulses at frequencies ω_1 and ω_2. The system is tuned by tuning the center frequency of one of the incident pulses (ω_2) and adjusting the phase matching of the nonlinear crystal switch.

tuned through a range of frequencies. Phase matching needs to be maintained over the desired tuning range by a suitable phase matching technique such as angular, temperature, or quasi phase matching. In the SFG method, high conversion efficiency requires that the two input pulses have a similar photon number and similar pulse intensities on the crystal, which can be impractical if the tunability of the input pulses is simultaneously sought. The DFG method (parametric amplification), however, utilizes the idler pulse for recirculation and requires only a single energetic, fixed-frequency input pulse (ω_1), accompanied by a tunable, low-energy seed pulse (ω_2). Such low-energy tunable pulse can be conveniently generated by the usual methods - tunable laser amplification, parametric generation and amplification, or optical parametric oscillation. This would be ideally done by using a fraction of the energy of the incident pulse ω_1 to ensure the consistency of $\omega_{1,2}$ inter-pulse timing, as shown in Fig. 12.

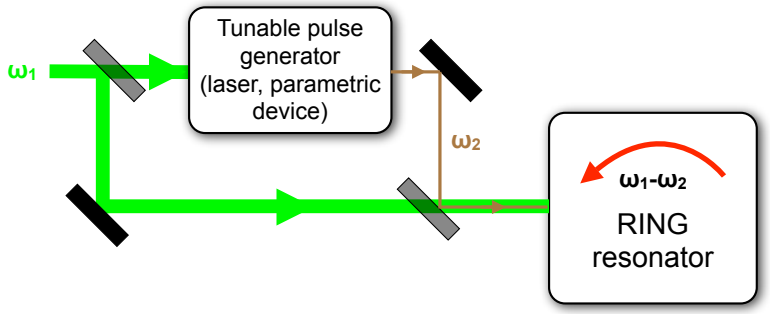

Fig. 12. Tunable RING using DFG. The synchronized tunable pulse at a frequency ω_2 can be generated by splitting a portion of the incident pulse ω_1 and pumping a tunable pulse generator based on a laser or a parametric process.

Intra-cavity spontaneous parametric generation of the tunable pulse represents another possibility, but its angular divergence and energy stability would likely pose limitations. Practical implementation of this method could be also real-

ized in a non-collinear frequency mixing scheme, but in practice the complexity of this approach would increase due to the pointing variation and angular dispersion of the resulting injected pulse and by possible requirement for pulse front tilt of short input laser pulses.

Fig. 13 shows an example of how the method for production and recirculation of pulses with tunable frequencies described above could be adapted to simultaneously recirculate pulses at multiple frequencies by SFG or DFG between the incident pulse at frequency ω_1 and two input pulses at frequencies ω_2 and ω_3. The DFG process produces two energetic pulses at frequencies $\omega_1 - \omega_2$ and $\omega_1 - \omega_3$, which are subsequently recirculated.

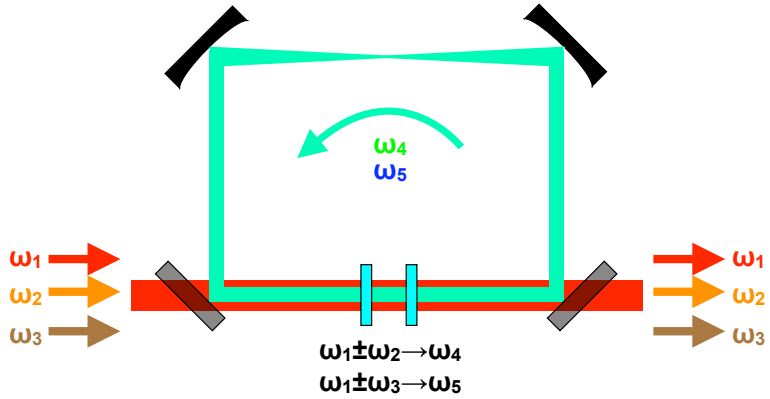

Fig. 13. Polychromatic RING recirculation could be realized by SFG or DFG between the input pulses at frequency ω_1 and two additional input pulses at frequencies ω_2 and ω_3.

In general, RING recirculation of an arbitrary number of pulses at variable frequencies $(\Omega_1 ... \Omega_m)$ can be accomplished by nonlinear frequency mixing of a suitable set of number of input pulses $(\omega_1 ... \omega_n)$ via any combination of the SFG or DFG scheme:

$$\begin{pmatrix} \Omega_1 \\ \Omega_2 \\ \dots \\ \Omega_m \end{pmatrix} = \begin{pmatrix} p_{11} & p_{12} & \dots & p_{1n} \\ p_{21} & p_{22} & \dots & p_{2n} \\ & & \dots & \\ p_{m1} & p_{m2} & \dots & p_{mn} \end{pmatrix} \begin{pmatrix} \omega_1 \\ \omega_2 \\ \dots \\ \omega_n \end{pmatrix}, \tag{10}$$

where $p_{ij} = \pm 1$.

8 Scaling prospects of the RING technique

One of the most attractive capabilities of the RING technique is its scalability to high-energy and high-peak-power pulse recirculation. In comparison, resonant coupling schemes exhibit limitations when scaled to higher energies both because of the absence of practical high-energy laser sources with repetition rates comparable to the typical cavity round-trip time on the order of ∼100 ns and because of the thermal effects associated with such pulses that complicate the interferometric alignment. In active switching schemes that rely on a linear switch such as an electro-optic (Pockels) cell, scaling to high energies entails the significant increase of the aperture to minimize accumulated nonlinear effects over the long (several cm) interaction length. This aperture increase is usually accompanied by a significant penalty in switching speed, which can become incompatible with cavity round-trip time.

The energy and peak power limitations of the RING technique are primarily driven by the nonlinear phase accumulation of the nonlinear crystal switch, and can be addressed by increasing the crystal aperture and length, as suggested in Section 4. Common nonlinear crystals available in large aperture and with optical quality to date include potassium dihydrogen phosphate (KDP) and its deuterated isomorph (KD*P), and can be obtained in sizes of up to 40 cm. If we assume the nonlinear drive of 10 GW/cm^2 with 10-ps pulses, this implies that a single crystal of this type could enable injection and recirculation of >100-J pulses. Furthermore, multiple nonlinear crystals could be tiled in an array to support much higher pulse energies. If required, coherence among beam components traversing different nonlinear crystals could be maintained by ensuring negligible thickness variation among crystals.

One of the possible limitations of the RING technique that could manifest itself at high repetition rates is the nonlinear crystal heating due to the increase in effective average power. The effective average power incident on the crystal can be approximated by

$$P_{eff} = P_0 \times A, \tag{11}$$

where P_{eff} is the effective average power present on the crystal, P_0 is the average power of the frequency converted pulse associated with the absence of the RING cavity, and A is the cavity enhancement factor, as defined in (4). This definition corresponds to the crystal thermal load primarily driven by linear absorption of the recirculating pulse. In practice, the average power experienced by the nonlinear crystal is slightly modified by the linear and nonlinear absorption of the input pulse and nonlinear absorption of the recirculated

pulse. Since nonlinear crystals to date have been used in applications producing average powers on the order of 1 kW, the expected thermal load from a 1-J, 10-Hz input pulse with a cavity enhancement factor of 100 is consistent with the thermal bandwidth and fracture limitations of nonlinear crystals. The thermal load is highly dependent on the crystal linear and nonlinear absorption and is generally increased at shorter wavelengths. The thermal management can be complicated by the small crystal thickness, which makes side cooling relatively inefficient. One of the possible thermal strategies to alleviate this issue is the use of the crystal in a reflection geometry, such that one of the crystal surfaces is contacted with a thick substrate which acts as a heat sink. This method can also lead to the reduction of the number of cavity surfaces and lower overall cavity Fresnel loss.

9 RING applications

The RING technique is attractive for use in applications that exhibit low loss for the laser pulse. A necessary but insufficient condition for this requirement is the low cross section (efficiency) for the interaction of interest. ICS of a laser pulse on a relativistic electron bunch is a prominent example of the process that exhibits both a low cross section for the useful interaction and simultaneously low loss for the laser pulse. Here we list some of the important applications that could benefit from the application of the RING technique.

For production of high (100 GeV-TeV) photon energies envisioned in the $\gamma-\gamma$ arm of the ILC [2] or for future intense positron sources [18], the required bunch structure consists of a set of 2820, $\sim$1-J, $\sim$1-ps micropulses spaced at 337 ns inside a macropulse at a repetition rate of 5 Hz. This bunch structure is very similar to the one potentially produced in an optimized RING recirculation system, and may lead to the reduction of the stringent requirements for the drive laser system energy and average power [14]. Since the γ-γ collider on ILC requires circular polarization in the interaction region, suitable implementation of linear-to-circular polarization conversion in the RING cavity is required.

In the intermediate (MeV) photon energy range, numerous applications based on ICS sources are being pursued and could benefit from the use of the RING technique. ICS has been recently proposed for production of highly monochromatic γ-rays for isotope-specific interrogation of shielded objects, with applications in nonproliferation, waste identification, material characterization, and homeland security [6]. The average brightness of the ICS source and the resulting interrogation times in this and other radiographic applications could be substantially shortened by the use of energetic laser pulse recirculation. Besides waste identification, another application in the nuclear fuel cycle that

has received significant attention is the waste transmutation utilizing nearly monoenergetic γ-rays produced by ICS. [4] In this area, significant work has been done on the use of very high-finesse cavities for efficient γ-ray generation. [19,20,21,22] This area could also potentially benefit from the use of the RING method for production of high-photon-number bursts of γ-rays.

In the low (keV) energy range, the application of ICS for production of monochromatic, directed x-rays for medical purposes has been pursued in the recent period, with a focus on medical diagnostics via K-edge imaging and radiological treatment via localized Auger cascade [7,8]. The brightness of such sources could be substantially improved by the use of the RING-like recirculation method, potentially resulting in reduced system cost and higher rate of imaging and treatment. In this x-ray energy range one can also envision applications of RING for production of ultrashort x-rays in synchrotron-based sources [23] for materials science and production of x-rays for lithography.

Other interesting applications that could benefit from the use of RING technique include plasma diagnostics by Thomson scattering, where efforts have been made to recirculate the pulse to obtain higher signal-to-noise ratio and possibly dynamical information [24], laser wire beam profile monitoring for electron beam diagnostics [25], Compton polarimetry [26], and the sensitive detection and measurement of the properties of gases and optical materials by pulsed cavity ring-down spectroscopy [27].

10 Conclusion

In conclusion, we proposed and experimentally demonstrated a novel high-peak-power laser pulse recirculation method highly suitable for applications involving ICS for high-energy, high-brightness x-ray or γ-ray beam generation. Our method, termed recirculation injection by nonlinear gating (RING), is uniquely capable of high-efficiency injection and trapping of a short, intense laser pulse required in those applications. The use of a nonlinear switch for pulse injection exhibits several important favorable characteristics, including the absence of interferometric alignment and timing requirements, compatibility with both the linear and ring cavity configurations, and the ability to generate and recirculate multiple laser pulses at the same or different center frequencies and repetition rates, thus opening up the possibility for tunable, shaped-pulse x-ray/γ-ray source.

The principal limitation of the RING technique in the simple implementation utilizing $\chi^{(2)}$ nonlinearities for pulse injection has been shown to be due to the accompanying $\chi^{(3)}$ nonlinearities, resulting in the change in focusing conditions and pulse spectral content. It has been shown that both limitations can be

addressed by the favorable scaling of the technique to greater apertures and longer nonlinear switch interaction lengths and by the design of the cavity for round-trip demagnification of the beam.

We believe the RING technique to be a strong alternative to resonant coupling techniques proposed and implemented to date for applications based on ICS, and foresee additional attractive applications in the area of ultrashort x-ray pulse generation, cavity ring-down spectroscopy and plasma diagnostics.

11 Acknowledgements

The authors wish to thank the U.S. Department of Energy Office of Nonproliferation Detection (NA-22) for financial support and technical guidance. We acknowledge valuable discussions with F. Hartemann, S. Bisson, and C. Haefner. This work was performed under the auspices of the U. S. Department of Energy by the University of California, Lawrence Livermore National Laboratory under Contract No. W-7405-Eng-48.

References

[1] P. Sprangle, A. Ting, E. Esarey, and A. Fisher, "Tunable, short pulse hard x-rays from a compact laser synchrotron source," J. Appl. Phys. **72**, 5032-5038 (1992).

[2] G. Klemz, K. Monig, and I. Will, "Design study of an optical cavity for a future photon-collider at ILC," Nucl. Instrum. Methods A **564**, 212-224 (2006).

[3] D. Li, K. Imasaki, and M. Aoki, "Analysis on coupling gamma-ray to nuclear giant resonance," J. Nucl. Sci. Technology **39**, 1247-1249 (2002).

[4] D. Li, K. Imasaki, M. Aoki, S. Miyamoto, S. Amano, K. Aoki, K. Hosono, and T. Mochizuki, "Experiment on gamma-ray generation and application," Nucl. Instrum. Methods A **528**, 516-519 (2004).

[5] D. Li, K. Imasaki, S. Miyamoto, S. Amano, and T. Mochizuki, "Experiment on photonuclear reaction induced by laser Compton scattering gamma ray," J. Nucl. Sci. Technology **42**, 259-261 (2005).

[6] J. Pruet, D. McNabb, C. A. Hagmann, F. V. Hartemann, and C. P. J. Barty, "Detecting clandestine material with nuclear resonance fluorescence," J. Appl. Phys. **99**, 123102 (2006).

[7] F. E. Carroll, M. H. Mendenhall, R. H. Traeger, C. Brau, and J. W. Waters, "Pulsed Tunable Monochromatic X-Ray Beams from a Compact Source: New Opportunities," Am. J. Roentgenology **181**, 1197-1202 (2003).

[8] F. E. Carroll, "Tunable, Monochromatic X-Rays: An Enabling Technology for Molecular/Cellular Imaging and Therapy," J. Cellular Biochemistry **90**, 502-508 (2003).

[9] F. V. Hartemann, W. J. Brown, D. J. Gibson, S. G. Anderson, A. M. Tremaine, P. T. Springer, A. J. Wootton, E. P. Hartouni, and C. P. J. Barty, "High-energy scaling of Compton scattering light sources," Phys. Rev. STAB **8**, 100702 (2005).

[10] D. J. Gibson, S. G. Anderson, C. P. J. Barty, S. M. Betts, R. Booth, W. J. Brown, J. K. Crane, R. R. Cross, D. N. Fittinghoff, F. V. Hartemann, J. Kuba, G. P. Le Sage, A. M. Tremaine, and P. T. Springer: "PLEIADES: a picosecond Compton scattering x-ray source for advanced backlighting and time-resolved material studies", Phys. Plasmas **11**, 2857-2862 (2004).

[11] D. Strickland and G. Mourou, "Compression of Amplified Chirped Optical Pulses," Opt. Comm. **56**, 219-221 (1985).

[12] W. P. Leemans, B. Nagler, A. J. Gonsalves, Cs. Tóth, K. Nakamura, C. G. R. Geddes, E. Esarey, C. B. Schroeder, and S. M. Hooker, "GeV electron beams from a centimetre-scale accelerator," Nature Physics **2**, 696-699 (2006).

[13] H. Schwoerer, B. Liesfeld, H.-P. Shlenvoigt, K.-U. Amthor, and R. Sauerbrey, "Thomson-Backscattered X Rays From Laser-Accelerated Electrons," Phys. Rev. Lett. **96**, 014802 (2006).

[14] J. Gronberg, "The NLC photon collider option progress and plans," Nucl. Instrum. Methods A **472**, 61-66 (2001).

[15] T. Mohamed, G. Andler, and R. Schuch, "Active optical storage ring for high-power laser pulses," Appl. Phys. B **79**, 817-821(2004).

[16] C. Gohle, T. Udem, M. Herrmann, J. Rauschenberger, R. Holzwarth, H. A. Schuessler, F. Krausz, and T. W. Hänsch, "A frequency comb in the extreme ultraviolet," Nature **436**, 234-237 (2005).

[17] T. Mohamed, G. Andler, and R. Schuch, "Development of an electro-optical device for storage of high power laser pulses," Opt. Commun. **214**, 291-295 (2002).

[18] P.L. Csonka, "Suggested Intense Positron Source based on (miropole) undulator induced pair production," Nucl. Instrum. Methods A **345**, 1-22 (1994).

[19] J. Chen, K. Imasaki, M. Fujita, C. Yamanaka, M. Asakawa, S. Nakai, and T. Asakuma, "Development of a high-brightness x-ray source," Nucl. Instrum. Methods A **341**, 346-350 (1994).

[20] M. Fujita, T. Asakuma, J. Chen, K. Imasaki, C. Yamanaka, M. Asakawa, N. Inoue, K. Mima, S. Nakai, T. Agari, N. Nakao, A. Moon, N. Ohigashi, T. Minamiguchi, Y. Tsunawaki, "POP expriments of the photon–e-beam interaction in the supercavity," Nucl. Instrum. Methods A **358**, 524-527 (1995).

[21] J. Chen, K. Imasaki, M. Fujita, C. Yamanaka, M. Asakuma, S. Nakai, and C. Yamanaka, "Compact high-brightness x-ray sources," Nucl. Instrum. Methods A **358**, 14-17 (1995).

[22] A. Moon, M. Fujita, E. Yasuda, H. Tanaka, P. K. Roy, M. Daicho, K. Ohkubo, N. Nakao, T. Watanabe, T. Ishida, K. Imasaki, N. Ohigashi, Y. Tsunawaki, K. Mima, S. Nakai, and C. Yamanaka, "Proof of principle experiments for Compton scattering of a stored photon in a supercavity," Jpn. J. Appl. Phys. **36**, L1446-1448)1997).

[23] R. W. Schoenlein, S. Chattopadhyay, H. H. W. Chong, T. E. Glover, P. A. Heimann, C. V. Shank, A. A. Zholents, and M. S. Zolotorev, "Generation of Femtosecond Pulses of Synchrotron Radiation", Science **287**, 2237-2240 (2000).

[24] M. Yu Kantor and D. V. Kouprienko, "High repetition rate probing laser for Thomson scattering diagnostics," Rev. Sci. Instrum. **70**, 780-782 (1999).

[25] H. Sakai, N. Sasao, S. Araki, Y. Higashi, T. Okugi, T. Taniguchi, J. Urakawa, and M. Takano, "Development of a laser wire beam profile monitor (2)", Nucl. Instrum. Methods A **455**, 113-118 (2000).

[26] I. Passchier, C. W. de Jager, N. H. Papadakis, N. P. Vodinas, D. W. Higinbotham, and B. E. Norum, A Compton Backscattering Polarimeter For Measuring Longitudinal Electron Polarization, Nucl. Instrum. Methods A **414**, 446458 (1998).

[27] A. O'Keefe and D. A. G. Deacon, "Cavity ring-down optical spectrometer for absorption measurements using pulsed laser sources," Rev. Sci. Instrum. **59**, 2544-2551 (1988).